

Anomalously Slow Domain Growth in Fluid Membranes with Asymmetric Transbilayer Lipid Distribution

Mohamed Laradji^{1,3} and P. B. Sunil Kumar^{2,3}

¹Department of Physics, The University of Memphis, Memphis, TN 38152

²Department of Physics, Indian Institute of Technology Madras, Chennai 600036, India

³MEMPHYS-Center for Biomembrane Physics, University of Southern Denmark, DK-5230, Denmark

The effect of asymmetry in the transbilayer lipid distribution on the dynamics of phase separation in fluid vesicles is investigated numerically for the first time. This asymmetry is shown to set a spontaneous curvature for the domains that alter the morphology and dynamics considerably. For moderate tension, the domains are capped and the spontaneous curvature leads to anomalously slow dynamics, as compared to the case of symmetric bilayers. In contrast, in the limiting cases of high and low tensions, the dynamics proceeds towards full phase separation.

PACS numbers: 87.16.-b, 64.75.+g, 68.05.Cf

Asymmetric distribution of lipids in the two leaflets of the plasma membrane is ubiquitous to many eukaryotic cells. Most of phosphatidylserine and phosphatidylethanolamine are located in the cytoplasmic leaflet, while sphingomyeline and phosphatidylcholine are predominantly in the outer leaflet [1]. This asymmetry, maintained by the cell through many active and passive processes, plays an important role in the lateral and trans-membrane compositional and morphological organizations in the nanometer scale. A very good example for such organization is the nanoscale domains, referred to as rafts. These domains are believed to be liquid-ordered regions, mainly composed of sphingomyelin, which is a saturated lipid, and cholesterol [2]. In spite of the wealth of experimental studies on lipid rafts, the mechanisms leading to their formation and their stability remain under intense debate. These issues are complicated by the presence of many components and processes in biomembranes.

With the aim to achieve the understanding of the physical properties of biomembranes, many experimental [3] and theoretical [4, 5] investigations have been carried out on relatively simple model lipid membranes. To the best of our knowledge, in all these studies, membranes have the same lipid composition in both leaflets of the bilayer. The natural next step in complexity towards the understanding of biomembranes is to consider membranes with different lipid composition in the two leaflets. An important question that arises is then: What role does this transbilayer asymmetry play on the domain structure of lipid bilayers? In particular, will this asymmetry result in a finite size of these domains? The purpose of the present paper is to address these questions using large scale dissipative particle dynamics (DPD) simulations.

Recent experiments clearly demonstrated that in multicomponent lipid vesicles there is a strong registration of the domains in the two leaflets. That is the type of lipids in the two leaflets are locally the same. This implies that, if there is a transbilayer asymmetry in the average lipid composition, these domains in register in the two leaflets will have to be of different areas. In order to minimize

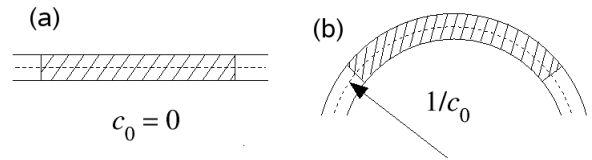


FIG. 1: (a) The configuration that minimizes the interaction energy between the lipids of a bilayer when the domains in the two layers are of the same area and (b) when the areas of the domains are different. The spontaneous curvature resulting from this area difference can be estimated by Eq. (1).

the interaction energy between unlike lipids the domains have to curve as shown schematically in Fig. 1. The area difference between the domains in the two leaflets should then give rise to a spontaneous curvature. This spontaneous curvature is only a function of the average compositions in the two leaflets, ϕ_{out} and ϕ_{in} defined as the number of A-lipids in the outer and inner leaflets, respectively, divided by the total number of lipids in the same leaflet

$$c_0 = \left(\frac{2}{\epsilon} \right) [(\phi_{out}/\phi_{in})^{1/2} - 1] / [(\phi_{out}/\phi_{in})^{1/2} + 1], \quad (1)$$

where, ϵ is the bilayer thickness.

Mean field calculations of multicomponent monolayer membranes, with curvature coupled to the local concentration through a spontaneous curvature, predict that when one of the components has a preferred curvature, the equilibrium state is that of caps or stripes. These calculations, considering an ordered patterns of domains, have been carried out both in two- [6, 7, 8, 9, 10] and three-component [8] monolayer models for lipid membranes. An ordered array of buds has also been proposed in the strong segregation limit [9, 10]. These calculations are performed on an infinite planar membrane. An extension of these calculations to the case of finite closed vesicles are difficult and have not yet been reported. It is important to note that the Hamiltonian used in these

monolayer models are based on a local bilinear coupling of the form, $\int_A \phi H$, where H is the local mean curvature and ϕ is the local composition field. One way to obtain these models from two-component bilayer models amounts to having a local mismatch between types of lipids in the outer and inner leaflets [7, 8], and therefore absence of domain register. Instead, a strong register reported in experiments suggests that it is more reasonable to expect a spontaneous curvature generated by the difference in area between the domains that are in register.

Motivated by the argument above, we carried out a systematic DPD simulation, of self-assembled lipid bilayer vesicles with different lipid compositions in the two leaflets of the bilayer. Within the DPD approach [14] a number of atoms or molecules are coarse-grained in order to form a fluid element, thereafter called a dpd particle. Specifically, we have in our case three types of beads, corresponding to a water-like bead, labeled w , a hydrophilic bead labeled h , representing a lipid head group, and a hydrophobic bead, labeled t , representing a group of CH_2 's in the tail group [15, 16]. The model parameters are selected such that the membrane is impermeable to the solvent thus allowing, in the case of a vesicle, to investigate the effect of conservation of inner volume. As in our previous study a lipid particle is modeled by a fully flexible linear amphiphilic chain, constructed from one hydrophilic h -particle, connected to three consecutive hydrophobic t -particles [4, 11]. There are two types of lipid particles, corresponding to A and B -lipids. The heads and tail dpd particles of an α -lipid, with $\alpha = A$ or B , are labeled h_α and t_α , respectively. The position and velocity of each dpd-particle are denoted by \mathbf{r}_i and \mathbf{v}_i , respectively. Within the DPD approach, all particles are soft beads that interact with each other through three pairwise forces corresponding to a conservative force, $F_{ij}^{(C)}$, a random force, $F_{ij}^{(R)}$, and a dissipative force, $F_{ij}^{(D)}$. The conservative force between dpd particles, i and j is given by $F_{ij}^{(C)} = a_{ij}\omega(r_{ij})\mathbf{n}_{ij}$ where $\mathbf{r}_{ij} = \mathbf{r}_i - \mathbf{r}_j$ and $\mathbf{n}_{ij} = \mathbf{r}_{ij}/r_{ij}$. Since all dpd particles are soft, we choose $\omega(r) = 1 - r/r_c$ for $r \leq r_c$, with r_c is the cutoff of interaction and is used to set a length scale in the simulations. $\omega(r) = 0$ for $r > r_c$. The integrity of a lipid chain is ensured through a simple harmonic interaction between consecutive monomers, $\mathbf{F}_{ij}^{(S)} = -C(1 - |\mathbf{r}_{ij}|/b)\mathbf{n}_{ij}$, where the spring constant $C = 100\epsilon$ and the length $b = 0.45r_c$. The dissipative force, describing friction between neighboring particles, is given by $\mathbf{F}_{ij}^{(D)} = -\gamma\omega^2(|\mathbf{r}_{ij}|)(\mathbf{n}_{ij} \cdot \mathbf{v}_{ij})\mathbf{n}_{ij}$, where $\mathbf{v}_{ij} = \mathbf{v}_i - \mathbf{v}_j$. Finally, the random force is given by, $\mathbf{F}_{ij}^{(R)} = -\sigma\omega(|\mathbf{r}_{ij}|)\zeta_{ij}(\Delta t)^{-1/2}\mathbf{n}_{ij}$ where ζ_{ij} is a random noise with zero mean and unit variance, and Δt is the time step of the simulation. The fluctuation-dissipation theorem requires that $\gamma_{ij} = \sigma_{ij}^2/2k_B T$. We used a fixed value for the parameter $\sigma_{ij} = \sigma$ for all pairs of dpd-particles. The head-head and tail-tail interactions between unlike lipids are given by $a_{h_A, h_B} = 50\epsilon$ and $a_{t_A, t_B} = 50\epsilon$ respectively with ϵ setting a scale for energy. All other parameters used in the present study are the same as in references [4, 11]. In our simulations,

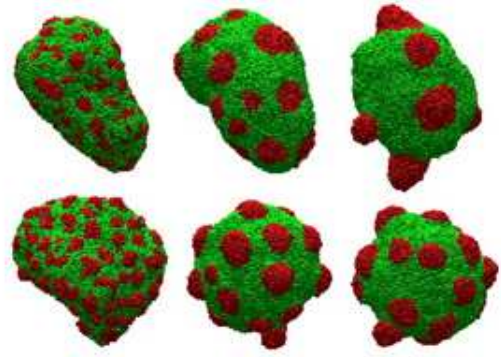


FIG. 2: Snapshot sequence of System II (bottom row) as compared to that of a symmetric vesicle having the same area to volume ratio (top row). Snapshots from left to right correspond to $t = 100, 2000$ and 4000τ , respectively.

a vesicle is composed of 16 000 lipid particles, embedded in a fluid consisting of 1 472 000 solvent particles with density $\rho = 3r_c^{-3}$, and the time step, $\Delta t = 0.05\tau$ [12] with $\tau = (mr_c^2/\epsilon)^{1/2}$ and m is the mass of a single dpd particle.

The interactions above ensure that the membrane is impermeable and that flip-flop events are extremely rare. The tail-tail interaction between two like lipids is less repulsive than that between two unlike lipids. Different tail-tail interactions are needed in order to mimic the fact that the hydrophobic region in domains which are rich in the saturated lipid and cholesterol is conformationally different from domains rich in unsaturated lipids. The phase separation is initiated through randomly labeling a fraction of all lipid particles as types A or B , such that the outer and inner leaflets have compositions ϕ_{out} and ϕ_{in} , respectively. The coarsening dynamics is then monitored through the computation of the cluster sizes of the minority lipid and the net interfacial length between the segregated domains. By simultaneously monitoring both interfacial length and the average domain area, we are able to investigate the physical mechanism via which domain growth proceeds.

Here, we present results for the case of $(\phi_{out}, \phi_{in}) = (0.4, 0.2)$ with three different area-to-volume ratios, corresponding to the case of the number of solvent particles in the vesicle's core, $N_s = 138000$ (System I), $N_s = 112400$ (System II), and $N_s = 72300$ (System III). In the remaining of this letter, the symmetric case, refers to a vesicle with $(\phi_{out}, \phi_{in}) = (0.3, 0.3)$ and an area-to-volume ratio equal to that in System II. In Fig. 2, a sequence of snapshots in the case of system II, with $(\phi_{out}, \phi_{in}) = (0.4, 0.2)$ are compared to that of a vesicle with symmetric transbilayer composition corresponding to $(\phi_{out}, \phi_{in}) = (0.3, 0.3)$. This figure clearly shows that the onset of domain capping is shifted to earlier times by the transbilayer asymmetry in the lipid composition, as opposed to the case of a symmetric vesicle. This capping result from the register between domains in the outer

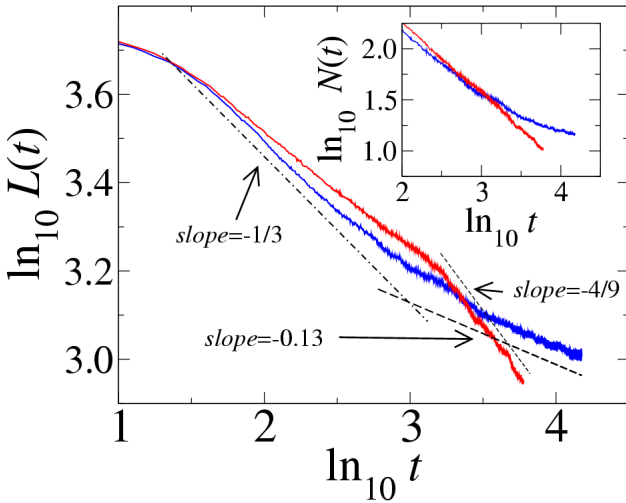


FIG. 3: Net interface length as a function of time. The data with the slope $-4/9$ corresponds to System II and that with slope -0.13 corresponds to the symmetric vesicle. Inset shows the net number of domains as a function of time for System II (top curve at late times) and for the symmetric vesicle (bottom curve).

and inner leaflets and mismatch between their areas (see Eq. (1)).

At late times the coarsening dynamics is slower in the asymmetric case than in the symmetric case as is evident from Fig. 2. This is substantiated by the time dependence of the net interface lengths of the two systems shown in Fig. 3. This slowing down is not observed in the symmetric case even during late times, which the expected fast growth law, $L \sim t^{-4/9}$, resulting from coalescence of caps [4]. Note that while the curvature of domains in the symmetric case is set by the competition between line tension and bending modulus [5], in the asymmetric case it is induced by the spontaneous curvature resulting from the asymmetry in the compositions of the two leaflets, and is set at early times (see Fig. 2). The late times slowing down shown in Fig. 3, must be the result of this spontaneous curvature. It is interesting to note that during the late stages, the interfacial length has a very small growth exponent (~ -0.13), indicative of a logarithmic growth. This is normally attributed to microphase separation, ubiquitous to many other soft materials [17]. This non-algebraic slow dynamics is the result of the competition between interfacial tension, which is the driving force of the phase separation, and an effective long-range repulsive interaction. In the present case this repulsive interaction should result from the combined effect of spontaneous curvature and lateral tension. Microphase separation in multicomponent lipid bilayers with spontaneous curvature has been predicted by mean field theories both in the weak and

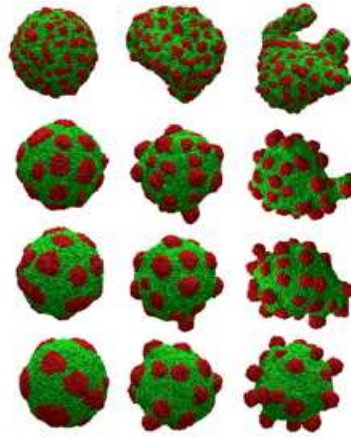


FIG. 4: Snapshot sequences for the three area to volume ratios considered in the present study. Rows from top to bottom represent the Systems-I, II, and III, respectively. Snapshots from left to right, in each row, correspond to times $t = 100$, 1000 , 2000 , and 5000τ , respectively.

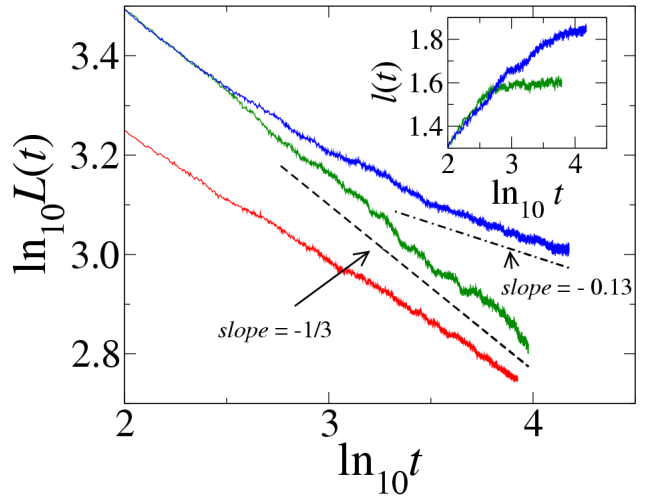


FIG. 5: Net interface length versus time. Curves from bottom to top corresponds to Systems I (bottom), III (middle), and II (top), respectively. The data line for System I (bottom) has shifted downwards for clarity. Straight lines are guides to the eye. In the inset, the average interface length per domain is shown versus time in Systems II (top curve), and III (bottom curve).

strong segregation limits at low values of lateral tension [6, 7, 8, 9, 10]. We should note that these theories assume that domains, in the microphase separation regime, are organized into a regular lattice. However thermal fluctuations could easily destroy the long-range order of these domains. Indeed, in our simulation, we see a melt of caps instead of a regular lattice.

Surface tension is expected to play an important role

on the phase separation of multicomponent lipid membranes. In the case of closed and impermeable vesicles with conserved number of lipids, the role of surface tension is effectively played by the area-to-volume ratio. Experimentally, surface tension is controlled by an osmotic pressure between the inner and outer environments of the vesicle. In Fig. 4, snapshots of vesicles with asymmetric composition are shown for three different values of the area-to-volume ratio, corresponding to Systems I, II and III. At low tension (System III), the large amount of excess area allows domains to acquire a bud shape, such that interfaces of the corresponding domains in each leaflet are in register. Due to similar reasons, at intermediate tensions (System II) domains acquire a cap shape since the excess area available in this case is less than that in System III. At high tensions (System I), the lack of excess area prevents domains from curving, leading them to remain nearly flat throughout the phase separation process.

The net interface lengths of the domain structure versus time are shown in Fig. 5 for the three different tensions. This figure shows that during early times of the phase separation process, i.e. for $t \lesssim 250$ the dynamics is independent of tension. As demonstrated by the early time configurations in Fig. 4, this is due to the fact that during this regime, domains are flat, and the composition dynamics is decoupled from the membrane curvature dynamics. At late stages, the dynamics in the three systems become noticeably different. We notice in particular that the dynamics is very slow in the case of intermediate tension (System II), as discussed above. In contrast, domain coarsening is faster and algebraic for both high (System I) and low (System III) tension, implying an approach towards full phase separation. A growth law, $L(t) \sim t^{-1/3}$ in System I, is the result of coalescence of flat domains as is shown earlier in Refs. [4, 11]. Our results for cases of intermediate and high tensions are in agreement with recent theoretical predictions [10]. However, for the low tension case, we see growth dynamics towards full phase separation. The equilibrium state here will be a completely phase separated vesicle [18].

The diffusion coefficient of a single bud should scale as $D \sim 1/a^{1/2}$, where a is the area of a single bud. If domain coarsening at late stages of system III is mediated by coalescence of spherical buds, with a fixed neck radius l , diffusing on the surface of the vesicle (the length scale here being set by the ratio of difference in area occupied by the B phase to the bilayer thickness) then the net interface length, $L(t) = N(t)l \sim t^{-2/3}$, where N is the total number of buds on the vesicle [13]. This growth law is much faster than what is shown in Fig. 5. $l(t) = L(t)/N$ for Systems II and III plotted in the inset of Fig. 5. This figure shows that the interfacial length per bud, and hence the neck radius, in system III reaches saturation at about $t \approx 250\tau$. A close examination of snapshots at late times clearly indicate that domain growth in system III is mediated by coalescence. Therefore, in order to reproduce the observed time dependence, $L(t) \sim t^{-1/3}$, the buds must move with an effective diffusion coefficient that scales as $1/a^2$. Since this is unrealistic there must be another process opposing the necks of two buds from merging. The details of this process is currently under investigation.

In conclusion, we examine the effect of transbilayer asymmetry in the lipid composition on phase separation. We found that at intermediate tension, the asymmetry leads to anomalously slow coarsening of caps, in agreement with recent mean field calculations. At low or vanishingly small lateral tension, where the domain structure is that of buds, and at high tension, where the domains are flat, we found algebraic domain growth leading to full phase separation. It would be very useful to explicitly correlate the nature of domain growth, with asymmetric transbilayer lipid distribution, with the surface tension of the membrane. We plan to perform the calculations of the surface tension in the various regimes from the lateral stress profiles using the approach similar to that in Refs. [16, 19].

M.L. thanks the Petroleum Research Fund and P.B.S.K. thanks the DST, India, for support. MEMPHYS is supported by the Danish National Research Foundation. Parts of the simulation were carried at the Danish Center for Scientific Computing.

[1] *Physics and the architecture of cell membranes* (Adam Hilger, Bristol, 1987); *Molecular Biology of the Cell* (3rd Ed.) by B. Alberts *et al.* (Garland Publishing, New York, 1994).

[2] A. Kusumi *et. al.*, *Traffic* **5**, 213 (2004); S. Mayor and M. Rao, *Traffic* **5**, 231 (2004).

[3] S.L. Veatch and S.L. Keller, *Phys. Rev. Lett.* **94**, 148101 (2005); C. Dietrich *et al.*, *Biophys. J.* **80**, 1417 (2001); S.L. Veatch and S.L. Keller, *Phys. Rev. Lett.* **89**, 268101 (2002); T. Baumgart, S.T. Hess, and W.W. Webb, *Nature (London)* **425**, 821 (2003); Bernadino de la Serna *et. al.*, *J. Biol. Chem.* **279**, 40715 (2004).

[4] M. Laradji and P.B. Sunil Kumar, *Phys. Rev. Lett.* **93**, 198105 (2004).

[5] *Structure and Dynamics of Membranes*, R. Lipowsky and E. Sackmann (Eds.) (Elsevier, Amsterdam, 1995).

[6] D. Andelman, T. Kawakatsu, and K. Kawasaki, *Europhys. Lett.* **19**, 57 (1992); Y. Jiang, T. Lookman, and A. Saxena, *Phys. Rev. E* **61**, R57 (2000); E.J. Wallace, N.M. Hooper, and P.D. Olmsted, *Biophys. J.* **88**, 4072 (2005).

[7] P.L. Hansen, L. Miao, and J.H. Ipsen, *Phys. Rev. E* **58**, 2311 (1998).

[8] P.B. Sunil Kumar, G. Gompper, and R. Lipowsky, *Phys. Rev. E* **60** 4610 (1999).

[9] W.T. Góźdż and G. Gompper, *Europhys. Lett.* **55**, 587 (2001).

[10] J.L. Harden, F.C. MacKintosh, P.D. Olmsted, *Phys. Rev. E* **72**, 011903 (2005).

[11] M. Laradji and P.B. Sunil Kumar, *J. Chem. Phys.* **123**,

224902 (2005).

- [12] A.F. Jakobsen, O.G. Mouritsen, and G. Besold, *J. Chem. Phys.* **122**, 204901 (2005).
- [13] P.B. Sunil Kumar, G. Gompper, and R. Lipowsky, *ibid.* **86**, 3911 (2001).
- [14] P.J. Hoogerbrugge and J.M.V.A. Koelman, *Europhys. Lett.* **19**, 155 (1992); P. Espagnol and P. Warren, *Europhys. Lett.* **30**, 191 (1995); P. Espagnol, *Europhys. Lett.* **40**, 631 (1997).
- [15] S. Yamamoto and S.-A. Hyodo, *J. Chem. Phys.* **118**, 7893 (2003); M. Venturoli, B. Smit, and M.M. Sperotto, *Bio-phys. J.* **88**, 1778-1798 (2005).
- [16] G. Ilya, R. Lipowsky, and J.C. Shillcock, *J. Chem. Phys.* **122**, 244901 (2005)
- [17] M. Laradji *et. al.*, *Adv. Chem. Phys.* **LXXXIX**, 159 (1994).
- [18] F. Jülicher and R. Lipowsky, *Phys. Rev. E* **53**, 2670 (1996).
- [19] J.C. Shillcock and R. Lipowsky, *J. Chem. Phys.* **117**, 5048 (2002); R. Goetz and R. Lipowsky, *J. Chem. Phys.* **108**, 7397 (1998).